From Nonlinear NDT to Conventional Ultrasonic Testing Techniques

Martin SCHNEIDER[1]
[1] Karlsruhe Institute of Technology (KIT), Karlsruhe, Germany

Abstract. The bottleneck problem of nonlinear NDT is a low efficiency of conversion from fundamental frequency to nonlinear frequency components. In this paper, it is proposed to use a combination of nonlinearity with Local Defect Resonance (LDR) to enhance substantially the input-output conversion. Since LDR is an efficient resonance "amplifier" of the local vibrations, it manifests a profound nonlinearity even at moderate ultrasonic excitation level. As the driving frequency matches the LDR-frequency band, a strong enhancement of the higher harmonic amplitudes generated locally in the defect area is observed. Besides a strong higher harmonic response, a high quality factor of LDR can also be used for efficient frequency mixing nonlinear NDT.

The "conventional" nonlinear effects, like higher harmonic generation and wave mixing are not the only dynamic scenario of nonlinear phenomena for resonant defects. At higher level of excitation, a combined effect of LDR and nonlinearity results in qualitatively new features characteristic of nonlinear and parametric resonances. Under resonance conditions nearly total input energy at fundamental frequency can be converted into higher harmonic or subharmonic vibrations of the defects. Both super- and subharmonic LDR are strongly localised in the defect area that provides a background for highly-sensitive defect-selective imaging. LDR mode of nonlinear NDT requires much lower acoustic power to activate nonlinearity of defects that makes it possible to avoid high-power ultrasonic instrumentation and switch to conventional ultrasonic equipment instead.

Introduction

The majority of ultrasonic instruments widely used in industry and technology for material characterization and quality assessment make use of a linear elastic response of materials that generally results in the amplitude and phase variations of the input signal. The nonlinear approach to ultrasonic NDT is concerned with nonlinear material response, which is inherently related to the frequency changes of the input signal. It is based on nonlinear behaviour of the defects with non-bonded contacts (cracks, delaminations, impacts, etc.) attributed to the so-called Contact Acoustic nonlinearity (CAN) [1]. The two CAN mechanisms are concerned with bimodular deformation of the material with defects: "clapping" of contact planes (for vibrations normal to the interface) and nonlinear friction between the contact surfaces for tangential vibrations. As a result, for a monochromatic ultrasonic input, the spectrum of defect vibrations acquire additional nonlinear spectral components like, higher harmonics (HH), subharmonics, mixing frequencies, etc., which are used as sensitive frequency "tags" of the damage presence in materials and components. Besides, these new frequency components are localized tightly in the defect areas and, therefore, serve as a background of defect-selective imaging of defects.

However, a long term bottleneck problem identified on the way of applications of nonlinear NDT is concerned with low efficiency of conversion from fundamental frequency to nonlinear frequency components. To proceed with a reliable nonlinear experiment one has simultaneously to take care of generating of a high-intensity (in the range of a few acoustic W) probing wave and detecting the faint nonlinear frequency signals produced in the material. This makes the experimental implementation of the nonlinear techniques very peculiar: they require a high-voltage (kV) very "clean" (klirr factor < 10^{-2}) electric input to

a “linear” transducer combined with sensitive (μV) receivers and a chain of various high- and low-pass filters.

The intention of this paper is to indicate the way of enhancing efficiency of the nonlinear frequency conversion by the vibrating defects. To this end, the nonlinearity of defects is combined with their resonance properties using the concept of Local Defect Resonance (LDR) [2, 3]. The LDR-based ultrasonic activation of defects enables to eliminate the high-intensity inputs and use “conventional” ultrasonic waves (with intensities in the mW range) instead. It would also avoid the instrumental specificity (both electronic units and transducers) of the nonlinear experiments and NDT applications aimed at detecting and imaging of localised defects.

1. Enhancement of nonlinearity via LDR

1.1 Higher Harmonic LDR Mode

Since LDR is as an efficient resonant “amplifier” of the local vibrations, one would expect it to contribute appreciably to material nonlinearity. To begin with the study of LDR effect on nonlinearity, a circular flat bottomed hole (FBH) defect (thickness 0.8 mm; radius 1 cm) in a typical low-nonlinear material PMMA with the LDR frequency response at 11 kHz was measured. A scanning laser vibrometer in particle velocity mode was used to monitor the LDR vibration pattern, waveform and the spectrum including HH.

The experimental results in Fig. 1 show that even such “linear” defects, like FBH in PMMA, turn into strongly nonlinear provided the driving frequency matches the LDR (11 kHz). For realistic defects, the higher background nonlinearity (CAN) combined with LDR results in an extremely efficient HH generation (Fig. 2). A crucial role of the driving frequency match to LDR for nonlinearity increase is illustrated in Figs. 3 and 4, correspondingly, for a delamination in glass fibre-reinforced (GFRP) plate and a crack in a unidirectional (UD-) CFRP rod. As the driving frequency matches the LDR frequencies, a strong enhancement ~20-40 dB of the HH amplitudes generated locally in the defect area is observed (Figs. 3, 4).

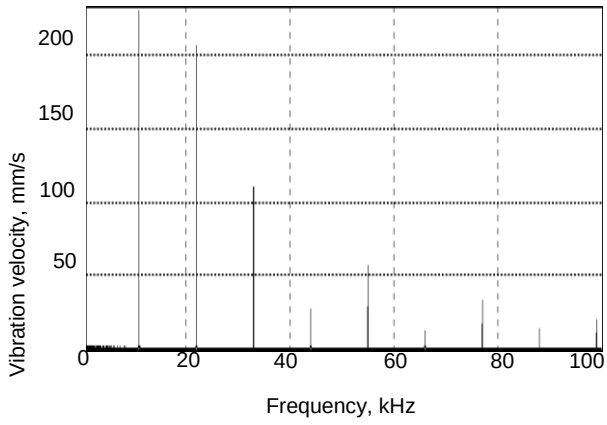

Fig. 1. HH spectra of FBH in PMMA specimen driven at LDR frequency 11 kHz.

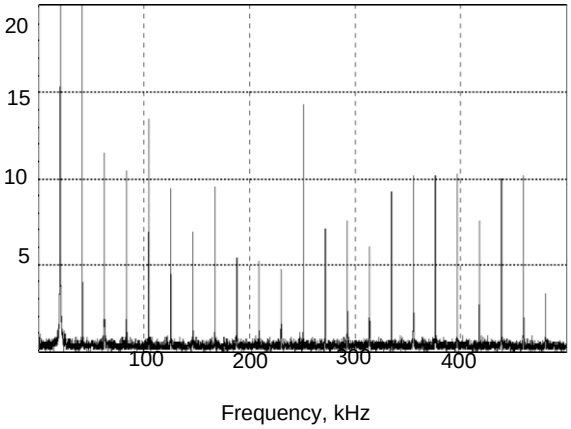

Fig. 2. HH spectrum for delamination in GFRP specimen driven at LDR frequency 20900 Hz.

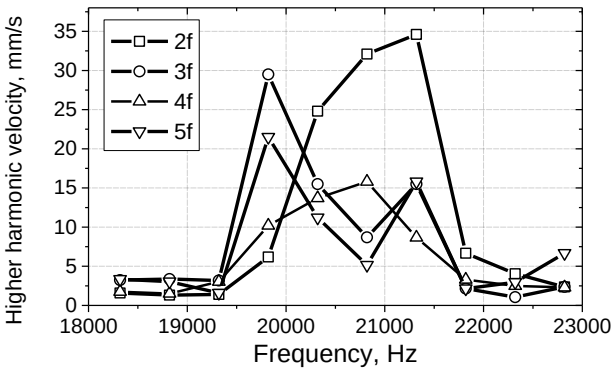

Fig. 3. Higher harmonic LDR frequency responses of a delamination in GFRP plate (LDR 20900 Hz).

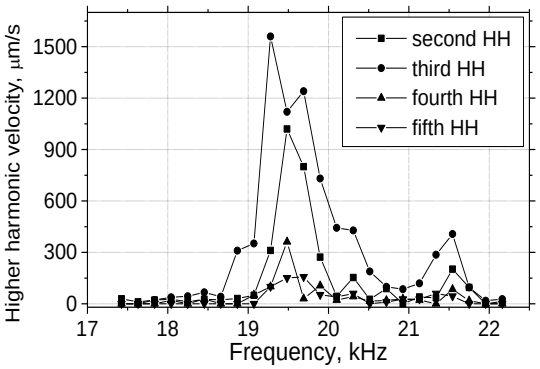

Fig. 4. Higher harmonic LDR frequency responses of a crack in UD-CFRP rod (LDR 19.5 kHz).

1.2. Frequency Mixing Modes

The method is based on the nonlinear interaction of ultrasonic waves of different frequencies (f_1, f_2) that results in a combination frequency output: $f_{\pm} = f_1 \pm f_2$. It is characterized by a lower spurious signal level than the HH mode and thus is prospective for NDT applications. A high-Q factor of LDR can be used to enhance the output signal of a combination frequency or the amplitudes of the interacting waves by matching to the LDR frequency response.

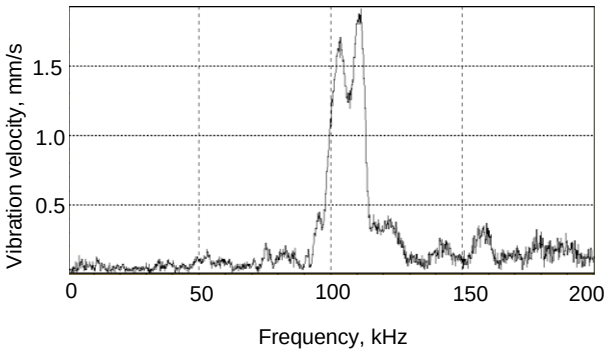

Fig. 5. LDR frequency response for an impact induced damage in a CFRP plate.

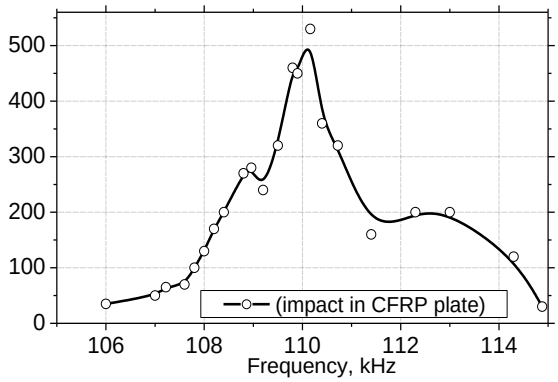

Fig. 6. LDR induced amplification at the sum frequency vibration for impact damage in CFRP plate.

An application of LDR as the “combination frequency amplifier” for NDT and imaging of realistic defects is illustrated then in Figs. 5 & 6 for an impact-induced damage (area ~5x5 mm^2) in the CFRP plate (280x40x1 mm^3). A linear LDR frequency response of the impact demonstrates a well-defined double-maxima peak around 110 kHz (Fig. 5). In the experiment, the two interacting flexural waves were excited in a continuous wave mode by the piezo-transducers attached to the opposite edges of the plate. One of the frequencies was fixed at $f_1 = 77.5$ kHz while the other was swept from $f_2 = 28.5$ to 37.5 kHz to provide the sum frequency variation around the LDR frequency of the defect. The vibration velocity amplitudes at f_1, f_2 and f_+ were monitored in the centre of the defect with a laser scanning vibrometer (vibration velocity mode). Fig. 6 shows the normalized velocity amplitude at sum frequency as a function of f_+ measured by changing f_2 in the frequency range indicated above. The impact of LDR is clearly seen by comparing the data with those

in Fig. 5: more than 20 dB increase in the output is observed when the combination frequency matches the frequency of LDR.

Another option of LDR mixing ("interacting waves amplifier") is illustrated in Figs. 7 &8. In the experiment, the impact damage with frequency response shown in Fig. 5 is insonified by the contra-flowing flexural waves. The frequency of one of the waves ($f_1 = 111500$ kHz) was chosen inside the LDR band while the frequency of the second wave (f_2) was swept within 80-130 kHz bandwidth. The spectrum of LDR vibrations (Fig. 7) is highly sensitive to the frequency match between f_2 and LDR (Fig. 8) so that multiple mixed frequency components are generated only as soon as both frequencies are inside the LDR band. The spectrum is well described by $mf_1 \pm nf_2$ combination produced by the $(m+n)$-order of nonlinear interaction. The side-lobe pattern in Fig. 7 reveals that the nonlinear interactions up to the 10th –order are developed by combining CAN and LDR.

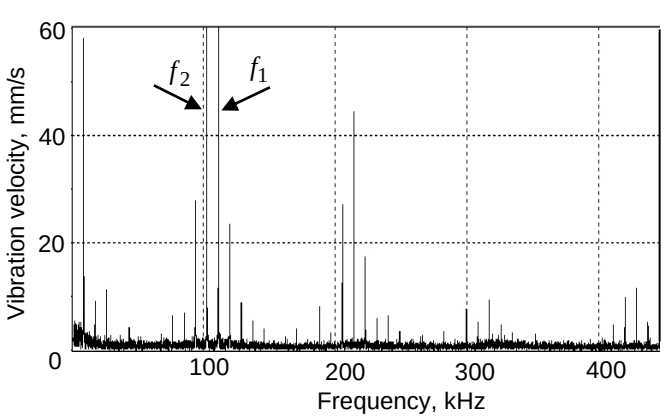

Fig. 7. Mixing frequency spectrum in an impact damage in a CFRP plate: $f_1 = 111500$ Hz; $f_2 = 102800$ Hz.

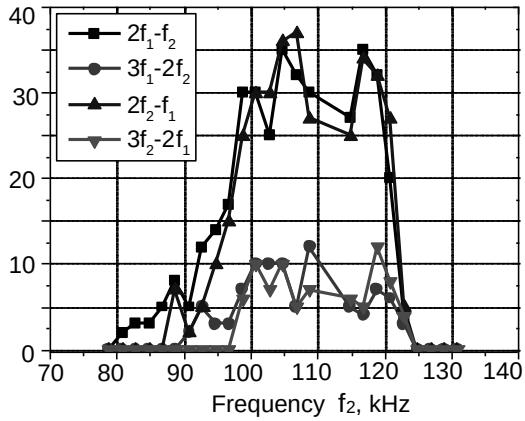

Fig. 8. Variation of mixed frequency amplitudes as functions of f_2 frequency swept around LDR.

1.3. Parametric LDR Modes

The results presented in Figs. 1-8 prove that at moderate input signals the LDR enhances appreciably the nonlinearity of defects via local "amplification" of vibrations. It raises substantially the efficiency of "conventional" nonlinear effects, like HH generation and frequency mixing. However, this is not the only dynamic scenario of nonlinear phenomena for resonant defects. At higher level of excitation, a combined effect of LDR and nonlinearity results in qualitatively new features characteristic of nonlinear and parametric resonances [4]. Manifestation of parametric effects (resonant growth of super- and subharmonic vibrations) is due to the amplitude-dependent shift (modulation) of LDR frequency induced by the driving signal. Unlike conventional (linear) resonance, the parametric resonances provide an exponential growth of the vibration amplitudes (instability) in time even in the presence of damping.

1.3.1. Superharmonic LDR Mode

For the superharmonic resonance, the input frequency is taken as a fraction ω_0 / n of the LDR frequency ω_0 and converted into ω_0 drive via the nth-order nonlinearity of the defect. A direct proof of superharmonic resonances in defects is demonstrated for the impact damaged CFRP specimen with LDR around 5140 Hz in Fig. 9. A one-half driving frequency (2570 Hz) was therefore selected for the excitation. To overcome parametric threshold, the input voltage was increased up to 60 -70 V. The spectrum (Fig. 9, a) and the

vibration pattern (Fig. 9, b) measured in the defect area beyond the threshold (65 V input) illustrate the dominance of the second harmonic vibration (period ~0.19 ms in Fig. 9, b). Because of the high-Q fundamental LDR, the superharmonic resonance required quite precise half-frequency placing within (10-20) Hz.

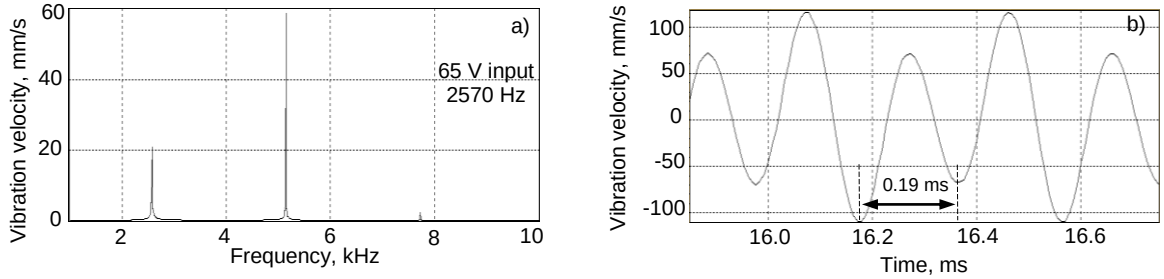

Fig. 9. Second-order superharmonic LDR for impact damage in CFRP: spectrum (a); vibration pattern (b).

Even higher frequency conversion efficiency is observed by using the third-order nonlinearity of the defect. One-third of the LDR frequency (1714 Hz) was therefore selected for the excitation while the input voltage was increased up to 80 V. The spectrum (Fig. 10) measured in the defect area illustrates the dominance of the third harmonic vibration (25 dB higher than the fundamental, Fig. 10) also proved by quite "clean" third harmonic vibration pattern (period ~0.19 ms in Fig. 11). Because of the high-Q fundamental LDR, the superharmonic resonance required quite precise one-third of LDR frequency placing within 100 Hz.

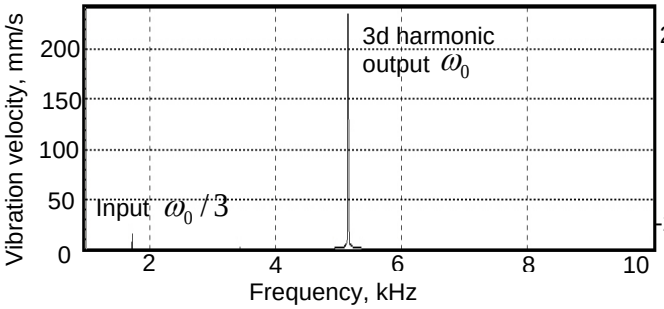

Fig. 10. Spectrum of the third-order superharmonic LDR in impact damaged CFRP plate.

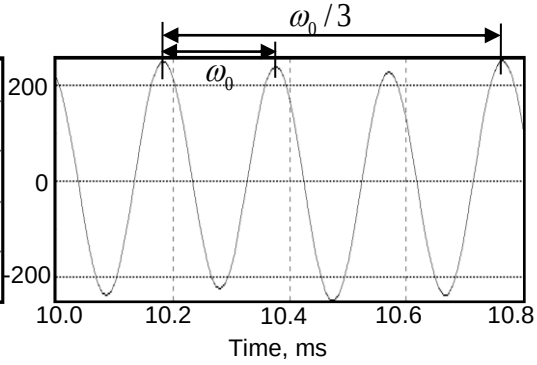

Fig. 11. Vibration pattern of the third-order superharmonic LDR in impact damaged CFRP plate.

1.3.2. Subharmonic LDR Mode

To observe a subharmonic resonance in the impact damaged CFRP specimen studied above, the excitation frequency was changed to the second harmonic (10280 Hz) frequency range of the fundamental LDR of the defect. Beyond $\approx$45 V threshold, the subharmonic component increases dramatically and prevails in the vibration (velocity) spectrum: $V_{\omega/2}/V_{\omega} \approx 30$ dB at 10275 Hz input (Fig. 12, a). This complies with pure sinusoidal subharmonic vibration pattern in the impact area beyond the threshold input (Fig. 12, b). The input frequency range for the subharmonic LDR was measured to be ~ 200 Hz, i.e. somewhat wider than that for the superharmonic counterpart.

The use of nonlinear LDR thus enables to amplify dramatically nonlinear response of defects. This suggests nonlinear LDR application as an efficient mode in nonlinear NDT. Besides, both super- and subharmonic LDR are strongly localized in the defect area that provides a background for the high-contrast defect-selective imaging.

2. LDR Defect-Selective Imaging

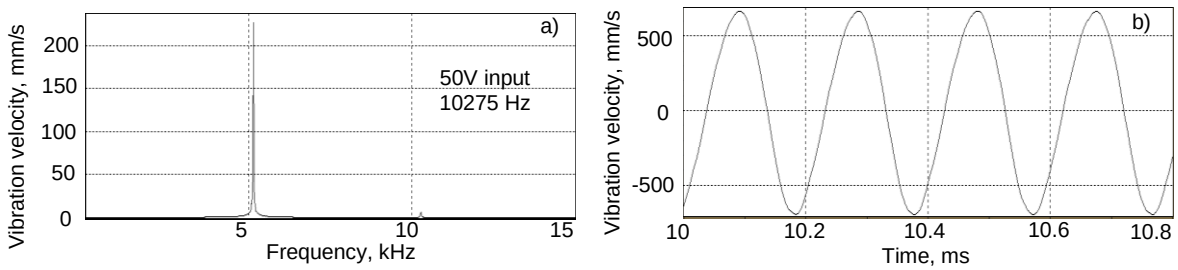

Fig. 12. Subharmonic LDR for impact damage in CFRP: spectrum (a) and vibration patterns (b).

A local "amplification" of the vibrations strictly confined in the defect area is a basis of a sensitive frequency-selective imaging even in a linear LDR case. The benefit of the linear LDR imaging is demonstrated in Fig. 13, where it is used for visualization of two small square artificial delaminations (8x8 mm^2 and 12x12 mm^2) with LDR frequencies 91130 Hz and 71250 Hz, correspondingly, in a CFRP plate (300x300x3 mm^3). The excitation at corresponding LDR frequencies results in imaging of the defects separately (Fig. 13 a, b) while a frequency sweep within the frequency range of both LDR brings a clear image of the both defects (Fig. 13, c).

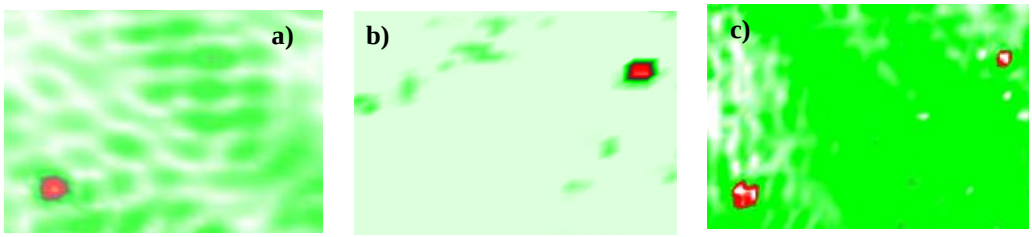

Fig. 13. Frequency-selective defect imaging of delaminations in CFRP plate in a linear LDR mode: excitation frequency 71250 Hz (a); 91130 Hz (b); frequency sweep 45-100 Hz (c).

By combining the resonance conditions provided by LDR with highly efficient elastic non-linearity (CAN) a substantial improvement in detecting and imaging of realistic defects can be expected. The benefit of the higher harmonic LDR imaging is illustrated in Fig. 14 & 16. A substantial improvement of the image quality was observed for the second harmonic LDR of 10x20 mm^2 delamination in 1 mm GFRP plate (Fig. 14, a): the signal-to-noise ratio (SNR) of the non-linear image in Fig. 14, c) is ~24 dB, while ~12 dB was measured at 36.77 kHz for the fundamental frequency LDR (b).

Another example in Fig. 15 demonstrates a high-quality image of a point impact in 5 mm thick CFRP window cut-out of an Airbus 350 (a) even in a linear LDR mode (b, c). However, the superior quality of the nonlinear imaging is noticeable in Fig. 15, d for the second HH mode.

As it was shown above, the efficient mixing frequency mode is observed when both frequencies of the probing waves are within the range of LDR frequency response. The test

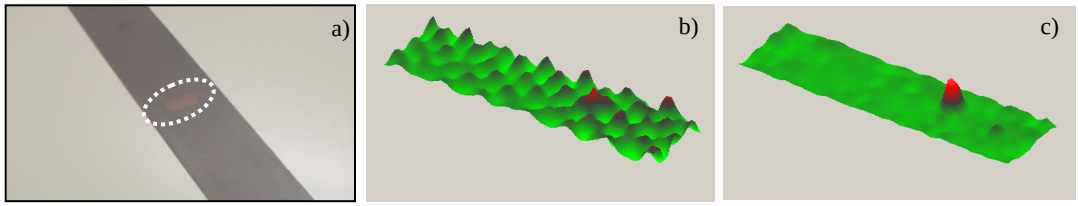

Fig. 14. Linear (36.77 kHz, b) and second harmonic (73.53 kHz, c) LDR imaging of a delamination in GFRP specimen (a).

in Fig. 16 is concerned with a crack in a CFRP plate whose LDR frequency is in the range of 37.5 ± 2.5 kHz (a). The defect is insonified with two oppositely propagating guided waves of the frequencies $f_1 = 36$ kHz and $f_2 = 38$ kHz. LDR amplified nonlinear interaction results in efficient combination frequency generation in the defect area (Fig. 16, b) which produce multiple images of the defect (c, d). The SNR of the images is found to depend on the order of interaction with maximum values ≈ 25 dB.

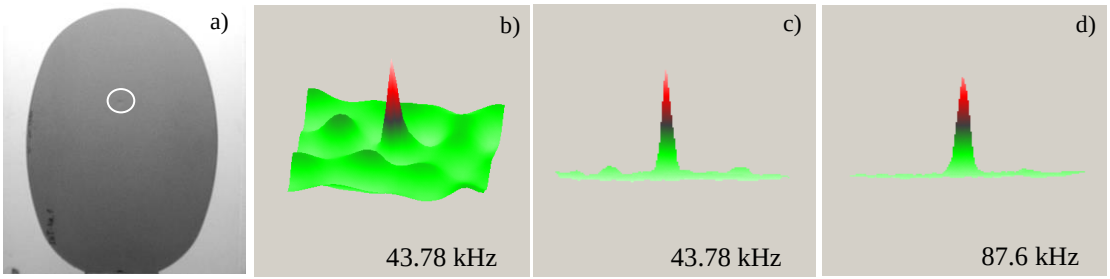

Fig. 15 A point impact damage in CFRP window of Airbus 350 (in a white circle (a), LDR frequency 43.78 kHz), its fundamental LDR images (b, c) and the second harmonic (87.6 kHz) image (d).

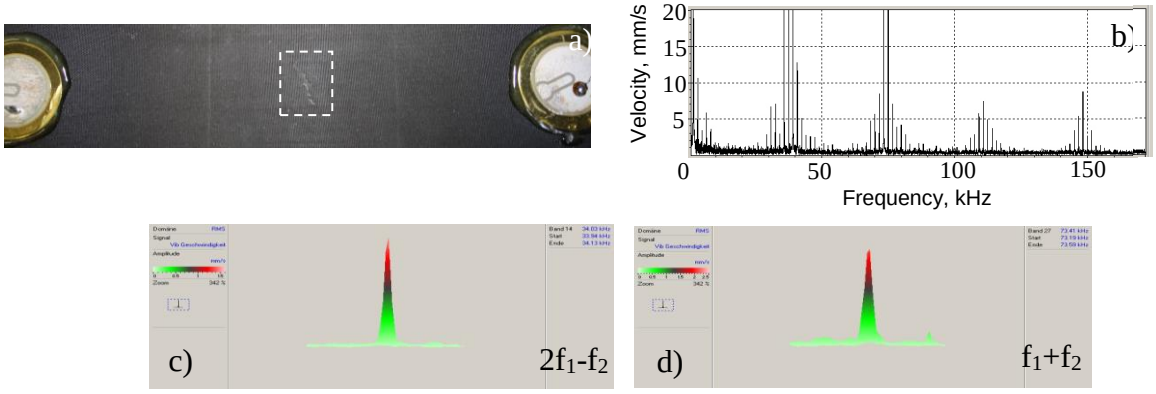

Fig. 16. Mixing frequency imaging of a crack in CFRP plate (a): Multiple frequency nonlinear spectrum (b) and two mixed frequency images (c, d).

Other examples of the resonance nonlinear imaging are given in Figs. 17 & 18. A drastic increase of the signal-to-noise ratio due to nonlinear LDR is readily seen from Fig. 17 for the third-order superhamonic resonance in the impact damaged CFRP specimen (LDR frequency 5145 Hz): for the excitation frequency at one third of the LDR frequency, the third harmonic results in ~17 dB SNR. Fig. 18 uses a subharmonic resonance for imaging of the impact damage in the same CFRP specimen: the specimen is excited at 10250 Hz and the subharmonic image is visualized at LDR frequency 5125 Hz with an excellent SNR ≥ 35 dB (Fig. 18).

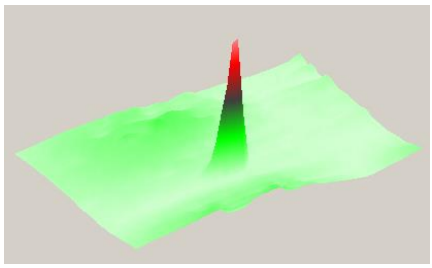

Fig. 17. Third-order superharmonic imaging of impact damage in CFRP: fundamental frequency 1715 Hz the image is at the third HH 5145 Hz.

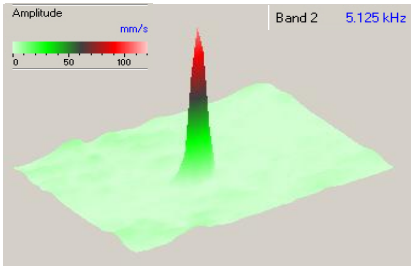

Fig. 18. Subharmonic LDR imaging of impact damage in a CFRP plate: Input 10250 Hz; output 5125 Hz.

3. Conclusions

A low efficiency of conversion from fundamental frequency to nonlinear frequency components is a long-term bottleneck problem impeding wider application of nonlinear ultrasonic techniques in NDT. In this paper, it is proposed to use a combination of both mechanical resonance and nonlinearity of defects to enhance substantially the input-output conversion.

Due to a strong resonant amplification of local vibrations, the defects manifest a profound nonlinearity even at moderate ultrasonic excitation level. As the driving frequency matches the LDR-frequency band, a strong enhancement (up to 40 dB) of the HH amplitudes generated locally in the defect area is observed. Besides a strong HH response, a high quality factor of LDR can also be applied for sensitive detection and imaging of defects in the frequency mixing modes.

The conventional nonlinear effects, like HH generation and wave mixing are not the only dynamic scenario of nonlinear phenomena for resonant defects. At higher level of excitation, a combined effect of LDR and nonlinearity results new nonlinear and parametric resonances. Under resonance conditions nearly total input energy at fundamental frequency can be converted into HH or subharmonic vibrations of the defects. Both super- and subharmonic LDR are strongly localised in the defect area that provides high-contrast defect- and frequency-selective imaging. A single imaging test in a resonant nonlinear mode results in multiple images of defects that enhances the probability of their detection, increase the signal-to-noise ratio, and improve the imaging quality.

The experiments prove viability of the resonant nonlinear methodology to detecting and imaging of various localized defects in composite materials (delaminations, impacts, cracks) for both laboratory-scale specimens and realistic aviation-related components. A crucial advantage of resonant nonlinear testing is concerned with dramatic reduction of ultrasonic power for activation of defect nonlinearity. The use of resonant nonlinear modes enables to avoid the instrumental specificity usually required for nonlinear testing and makes it compatible with conventional ultrasonic NDT methodologies.

Acknowledgement

The author acknowledges support of this study in the framework of ALAMSA project funded from the European Union's Seventh Framework Programme for research, technological development and demonstration under grant agreement no. 314768.

References

1. I Solodov, N Krohn, G Busse, “CAN: An example of nonclassical nonlinearity in solids**”,** Ultrasonics, Vol. 40, pp 621-625, 2002.
2. I Solodov, J Bai, S Bekgulyan, and G Busse, “A local defect resonance to enhance acoustic wave-defect interaction in ultrasonic nondestructive testing”, Applied Physics Letters, Vol. 99, 211911 2011.
3. I Solodov, J Bai, and G Busse, “Resonant ultrasonic spectroscopy of defects: Case study of flat-bottomed holes”, Journal of Applied Physics, Vol. 113, 223512, 2013.
4. I Solodov, “Resonant acoustic nonlinearity of defects for highly-efficient nonlinear NDE”, Journal of Nondestructive Evaluation, Vol. 33, pp. 252-262, 2014.